Mean-field equations for cigar- and disk-shaped Bose and Fermi superfluids

Camilo A. G. Buitrago and S. K. Adhikari

Instituto de Física Teórica, UNESP - São Paulo State University,
01.140-070 São Paulo, São Paulo, Brazil

Abstract.

Starting from the three-dimensional (3D) time-dependent nonlinear Gross-Pitaevskii equation for a Bose-Einstein condensate (BEC) and density functional (DF) equation for a Fermi superfluid at the unitarity and Bardeen-Cooper-Schrieffer (BCS) limits, we derive effective one- (1D) and two-dimensional (2D) mean-field equations, respectively, for the dynamics of a trapped cigar- and disk-shaped BEC and Fermi superfluid by using the adiabatic approximation. The reduced 1D and 2D equations for a cigar- and disk-shaped Fermi superfluid have simple analytic nonlinear terms and at unitarity produce results for stationary properties and non-stationary breathing oscillation and free expansion in excellent agreement with the solution of the full 3D equation.

PACS numbers: 05.60.Gg,05.30.Fk, 03.75.Kk, 71.10.Ay

1. Introduction

Many of the stationary and non-stationary properties of a trapped Bose-Einstein condensate (BEC) (or a Bose superfluid) can be satisfactorily explained by the mean-field Gross-Pitaevskii (GP) equation [1]. However, there is no such mean-field equation in configuration space for the Fermi superfluid even after the experimental realization of the crossover from the Bardeen-Cooper-Schrieffer (BCS) limit through unitarity to the Bose limit in a trapped Fermi superfluid [2, 3, 4, 5].

To study the properties of stationary and non-stationary states of a trapped Fermi superfluid with equal number of paired spin-up and -down fermions, Adhikari and Salashnich developed a Galilei-invariant nonlinear density functional (DF) equation valid from the weak-coupling BCS limit to unitarity [6, 7]. The solution of the DF equation of [6] yielded results for energy of a trapped Fermi superfluid in close agreement with those obtained from Monte Carlo calculations [8] not only in the BCS and unitarity limits but also along the BCS-unitarity crossover [2].

In actual experiments, an axially symmetric [1, 3, 9], rather than a spherical, trap is usually employed for the confinement of the BEC or Fermi superfluid. In many situations of actual interest, the trap has an extreme geometry [9], e.g., very strong radial or axial confinement. Consequently, the superfluid is formed in the shape of a cigar or a disk and the solution of the nonlinear equation in such cases deserves special attention. The cigar-shaped BEC or Fermi superfluid is quasi one dimensional (1D) and the reduction of the full three-dimensional (3D) equation to accurate 1D form would be of advantage. Similarly, it would be beneficial to reduce the full 3D equation to 2D form for the description of a disk-shaped BEC and Fermi superfluid.

We propose a simple scheme for the 3D-1D and 3D-2D reduction of the GP equation for a BEC and the DF equation for a Fermi superfluid at the BCS and unitarity limits. The 3D-1D reduction for a cigar-shaped BEC or a Fermi superfluid is done in the adiabatic approximation which assumes the essential dynamics to be confined in the axial direction with the radial degrees of freedom adjusting instantaneously to the minimum energy equilibrium configuration compatible with the axial dynamics [10, 11]. Under this approximation the 3D wave function factorizes into an explicitly time-dependent axial and time-independent radial parts which allows for a formal reduction of the original time-dependent 3D nonlinear equation into a time-dependent 1D and an auxiliary time-independent 2D equations. The same is also true for a disk-shaped BEC or a Fermi superfluid with the role of time-dependent 1D and auxiliary time-independent 2D equations interchanged, e.g., the time-dependent equation is now 2D and the auxiliary equation 1D in nature.

First we illustrate the present scheme through an application to a BEC described by the GP equation, where there are already several schemes [10, 11, 12, 13, 14, 15, 16, 17, 18, 19] for 3D-1D and 3D-2D reductions. Among these, the reduction schemes of Salasnich *et al.* (SPR) [10, 12] and Muñoz Mateo *et al.* (MMD) [11, 13] are the simplest to implement and have been shown to be the most efficient [11]. We compare the present

scheme with those of SPR [10, 12] and MMD [11, 13] for a BEC. Recently, Adhikari and Salasnich (AS) [20] suggested one scheme for such 3D-1D and 3D-2D reductions of the 3D DF equation for a Fermi superfluid at the BCS and unitarity limits. We apply our scheme to a Fermi superfluid and obtain distinct 3D-1D and 3D-2D reductions.

In section 2 we illustrate the 3D-1D and 3D-2D reduction schemes in the case of the GP equation for a BEC. In section 3 we consider the reduction schemes for the nonlinear DF equation of a Fermi superfluid at unitarity and BCS limits. In this case we reduce the 3D DF equation to 1D (for cigar-shaped superfluid) and 2D (for disk-shaped superfluid) forms with analytic nonlinear terms. We show that the reduced 1D and 2D equations for cigar- and disk-shaped Fermi superfluids are very effective for describing the stationary states and non-stationary breathing oscillation and free expansion of the Fermi superfluid at unitarity in close agreement with the solution of the full 3D DF equation. Finally, in section 4 we give a summary and some concluding remarks.

2. 3D-1D and 3D-2D Reductions of the GP equation

We first apply our approach to a BEC described by the GP equation. The GP equation for N bosons of mass m is written as [1]

$$\left[-i\hbar\frac{\partial}{\partial\hat{t}} - \frac{\hbar^2\nabla^2_{\hat{\mathbf{r}}}}{2m} + V(\hat{\mathbf{r}}) + \frac{4\pi\hbar^2\hat{a}N}{m}|\Psi(\mathbf{r})|^2\right]\Psi(\hat{\mathbf{r}},t) = 0, \tag{1}$$

with $\hat{a}$ the atomic scattering length, normalization $\int|\Psi|^2 d^3\hat{\mathbf{r}} = 1$, $V(\hat{\mathbf{r}}) = m\omega^2(\hat{\rho}^2 + \lambda^2\hat{z}^2)/2$ the harmonic trapping potential with frequencies ω and $\lambda\omega$ in radial ($\hat{\rho}$) and axial ($\hat{z}$) directions ($\hat{\mathbf{r}} \equiv \hat{\rho}, \hat{z}$). Employing dimensionless harmonic oscillator units $t = \hat{t}\omega, \mathbf{r} = \hat{\mathbf{r}}/a_\rho, z = \hat{z}/a_\rho, \rho = \hat{\rho}/a_\rho, a = \hat{a}/a_\rho, \psi = \Psi a_\rho^{3/2}, a_\rho = \sqrt{\hbar/m\omega}$, (1) can be written as

$$\left[-i\frac{\partial}{\partial t} - \frac{\nabla^2_{\mathbf{r}}}{2} + \frac{\rho^2+\lambda^2 z^2}{2} + 4\pi aN|\psi|^2\right]\psi(\mathbf{r},t) = 0, \tag{2}$$

with normalization $\int|\psi|^2 d^3\mathbf{r} = 1$.

In the limits of very small (cigar-shaped trap) and very large (disk-shaped trap) λ, the length scales in the axial and radial directions are very different. Consequently, the correlations between these two directions can be neglected and the condensate wave function could be factorized in variables ρ and z [10, 11]. In the case of cigar-shaped traps the dynamics takes place in the axial direction. The opposite happens in case of a disk-shaped trap. For a stationary solution $\psi(\mathbf{r})$ of (2) in a cigar-shaped trap one can define a linear density $\phi^2(z) \equiv \int d^2\rho\psi^2(\mathbf{r})$. Similarly, for a disk-shaped trap one can define a radial density $\varphi^2(\rho) \equiv \int dz\psi^2(\mathbf{r})$.

2.1. 3D-1D reduction for a cigar-shaped BEC

For a cigar-shaped trap, the above consideration leads to the factorization [11]

$$\psi(\mathbf{r},t) = \varphi(\rho, n_1(z,t))\phi(z,t), \tag{3}$$

where linear density n_1 is defined as $n_1(z,t) \equiv N|\phi(z,t)|^2 = N\int d^2\rho|\psi|^2$ and normalizations $\int d^2\rho|\varphi(\rho,n_1)|^2 = \int dz|\phi(z,t)|^2 = 1$. We *assume* that the function $\varphi(\rho,n_1(z,t))$ has no explicit t or z dependence and hence these derivatives do not act on this function. This is a good approximation, in general, as we find in numerical studies. The substitution of (3) in (2) then leads to

$$\varphi(\rho,n_1)\left[i\frac{\partial}{\partial t}+\frac{1}{2}\frac{\partial^2}{\partial z^2}-\frac{1}{2}\lambda^2z^2\right]\phi(z,t)=\phi(z,t)\left[-\frac{1}{2}\nabla_\rho^2+\frac{1}{2}\rho^2+4\pi an_1|\varphi|^2\right]\varphi(\rho,n_1). \quad (4)$$

Multiplying (4) by $\varphi^*(\rho,n_1)$ and integrating in ρ this equation can be rewritten as [11]

$$\left[i\frac{\partial}{\partial t}+\frac{1}{2}\frac{\partial^2}{\partial z^2}-\frac{1}{2}\lambda^2z^2-\mu_\rho(n_1)\right]\phi(z,t)=0, \quad (5)$$

$$\mu_\rho(n_1)=\int d^2\rho\varphi^*\left[-\frac{1}{2}\nabla_\rho^2+\frac{1}{2}\rho^2+4\pi an_1|\varphi|^2\right]\varphi, \quad (6)$$

where $\mu_\rho(n_1)$ is the chemical potential emerging from the 2D GP equation:

$$\left[-\frac{1}{2}\nabla_\rho^2+\frac{1}{2}\rho^2+4\pi an_1|\varphi|^2-\mu_\rho(n_1)\right]\varphi(\rho,n_1)=0. \quad (7)$$

We have decoupled the essential axial (z) and nonessential radial (ρ) degrees of freedom. The solution of the time-independent radial GP equation (7) leads to the chemical potential $\mu_\rho(n_1)$ given by (6), which is the nonlinear term of the axial GP equation (5).

The form of the chemical potential $\mu_\rho(n_1)$ of (7) is known in the small and large N limits. In the small N weak-coupling limit, the wave function can be approximated by the following normalized Gaussian form [21]

$$\varphi(\rho,n_1)=\exp[-\rho^2/(2\alpha^2)]/(\sqrt{\alpha^2\pi}), \quad (8)$$

where α is the width. With this wave form the chemical potential of (6) becomes

$$\mu_\rho(n_1)=\left(\frac{\alpha^2}{2}+\frac{1}{2\alpha^2}\right)+\frac{2an_1}{\alpha^2}. \quad (9)$$

In the large N Thomas-Fermi (TF) limit, as $an_1\to\infty$, the kinetic energy gradient operator in (7) can be neglected and this equation has analytic solution. The normalization condition of the TF wave function leads to [10, 11]

$$\mu_\rho(n_1)=\sqrt{4an_1}. \quad (10)$$

We suggest the following simple interpolation formula for $\mu_\rho(n_1)$ valid for small to large an_1 incorporating the limiting values (9) and (10)

$$\mu_\rho(n_1)=\frac{1}{2\alpha^2}-\frac{\alpha^2}{2}+\sqrt{\alpha^4+4an_1} \quad (11)$$

to be used in (5), where α is taken as a fixed constant for all n_1. In the weak-coupling $an_1\to 0$ limit, (7) reduces to the Schrödinger equation for a 2D harmonic oscillator with the exact solution (8) with $\alpha=1$. Then (11) is a good approximation to (6) for $\alpha=1$. For slightly larger values of an_1 (11) continues to be a good approximation to (6), but with a slightly smaller value of α. Motivated by this, we take a slightly smaller value of α in (11). For large an_1, (11) has the correct TF limit independent of the value of α

employed. This flexibility in introducing a width $\alpha \approx 1$ (slightly different from $\alpha = 1$) in (11) will be fundamental in making the 1D model equation (5) a faithful approximation to the 3D GP equation (2) for a cigar-shaped condensate for all an_1.

By construction, approximation (11) satisfies the weak-coupling and TF limits (9) and (10), respectively, for small and large an_1. The approximation of MMD is [11]

$$\mu_\rho(n_1) = \sqrt{1 + 4an_1}, \tag{12}$$

whereas SPR suggested [10]

$$\mu_\rho(n_1) = \frac{1 + 3an_1}{\sqrt{1 + 2an_1}}. \tag{13}$$

Here we calculate the chemical potential $\mu_\rho(n_1)$ of the three approaches and compare with the precise results for $\mu_\rho(n_1)$ obtained from a numerical solution of (7). (All numerical results presented in this paper are obtained with the imaginary-time propagation scheme after a discretization by the Crank-Nicholson method using the FORTRAN programs provided in [22], the details of which are described there. The numerical simulations for the dynamical breathing oscillation and free expansion for a Fermi superfluid at unitarity reported in Secs. IIIC and IIID, respectively, were performed with the real-time propagation scheme after a discretization by the Crank-Nicholson method.) Our finding is exhibited in table 1 for different an_1 and for $\alpha = 0.985$ together with those obtained from the MMD [11] and SPR [10] schemes.

Table 1. Chemical potential $\mu_\rho(n_1)$ of (6) for different an_1 obtained from an accurate numerical solution of (7), and from (11) (Present, $\alpha = 0.985$), (12) (MMD) [11], and (13) (SPR) [10].

an_1	Numerical	MMD	SPR	Present
0	1	1	1	1.00045
0.2	1.346427	1.34164	1.35225	1.34983
1	2.257135	2.23607	2.30940	2.25314
10	6.432456	6.40312	6.76475	6.42877
100	20.04320	20.0250	21.2309	20.0538

2.2. 3D-2D reduction for a disk-shaped BEC

For a disk-shaped trap the adiabatic approximation leads to the factorization [10, 11]

$$\psi(\mathbf{r}, t) = \varphi(\rho, t)\phi(z, n_2(\rho, t)), \tag{14}$$

where the surface density n_2 is defined as $n_2(\rho, t) \equiv N|\varphi(\rho, t)|^2 = N\int dz|\psi|^2$ and normalizations $\int d^2\rho|\varphi(\rho, t)|^2 = \int dz|\phi(z, n_2)|^2 = 1$. The substitution of (14) in (2) leads to

$$\phi(z, n_2)\left[i\frac{\partial}{\partial t} + \frac{1}{2}\nabla_\rho^2 - \frac{1}{2}\rho^2\right]\varphi(\rho, t) = \varphi(\rho, t)\left[-\frac{1}{2}\frac{\partial^2}{\partial z^2} + \frac{1}{2}\lambda^2 z^2 + 4\pi an_2|\phi|^2\right]\phi(z, n_2) \tag{15}$$

Multiplying (15) by $\phi^*(z, n_2)$ and integrating in z, this equation can be rewritten as the set of equations

$$\left[i\frac{\partial}{\partial t} + \frac{1}{2}\nabla_\rho^2 - \frac{1}{2}\rho^2 - \mu_z(n_2)\right]\varphi(\rho, t) = 0, \tag{16}$$

$$\left[-\frac{1}{2}\frac{\partial^2}{\partial z^2} + \frac{\lambda^2 z^2}{2} + 4\pi a n_2|\phi|^2 - \mu_z(n_2)\right]\phi(z, n_2) = 0, \tag{17}$$

$$\mu_z(n_2) = \int dz\phi^*\left[-\frac{1}{2}\frac{\partial^2}{\partial z^2} + \frac{\lambda^2 z^2}{2} + 4\pi a n_2|\phi|^2\right]\phi. \tag{18}$$

It is convenient to introduce scaled variables $\bar{z} = z/a_z$, $\bar{\phi} = \sqrt{a}_z\phi$, and $\bar{\mu}_z = \mu_z a_z^2$ with $a_z = \sqrt{1/\lambda}$, when (17) and (18) become

$$\left[-\frac{1}{2}\frac{\partial^2}{\partial \bar{z}^2} + \frac{\bar{z}^2}{2} + 4\pi a a_z n_2|\bar{\phi}|^2 - \bar{\mu}_z(n_2)\right]\bar{\phi}(z, n_2) = 0, \tag{19}$$

$$\bar{\mu}_z(n_2) = \int d\bar{z}\bar{\phi}^*\left[-\frac{1}{2}\frac{\partial^2}{\partial \bar{z}^2} + \frac{\bar{z}^2}{2} + 4\pi a a_z n_2|\bar{\phi}|^2\right]\bar{\phi}. \tag{20}$$

The form of the chemical potential $\bar{\mu}_z(n_2)$ of (19) is known in the small and large N limits. In the small N weak-coupling limit the wave function can be approximated by the following normalized Gaussian form [21]

$$\bar{\phi}(\bar{z}, n_2) = \exp[-\bar{z}^2/(2\eta^2)]/(\eta^2\pi)^{1/4}, \tag{21}$$

where η is the width. With this wave form the chemical potential of (20) becomes

$$\bar{\mu}_z(n_2) = \left(\frac{\eta^2}{4} + \frac{1}{4\eta^2}\right) + 2aa_z n_2\frac{\sqrt{2\pi}}{\eta}. \tag{22}$$

In the large N limit the normalization condition of the TF wave function leads to [11]

$$\bar{\mu}_z(n_2) = (3\pi a a_z n_2/\sqrt{2})^{2/3}. \tag{23}$$

For a disk-shaped BEC we suggest the following simple interpolation formula for $\bar{\mu}_z(n_2)$ incorporating the limiting values (22) and (23)

$$\bar{\mu}_z(n_2) = \frac{1}{4\eta^2} - \frac{(\pi - 1)\eta^2}{4} + \left[\left(\frac{\pi\eta^2}{4}\right)^{3/2} + \frac{3\pi a a_z n_2}{\sqrt{2}}\right]^{2/3}, \tag{24}$$

valid for all $aa_z n_2$, where η is taken as a fixed constant for all $aa_z n_2$. The flexibility in introducing a width η slightly different from 1 in (24) will make the 2D model equation (16) an accurate approximation to the 3D GP equation (2) for a disk-shaped condensate for all $aa_z^2 n_2$.

Instead of taking η as a constant, SPR [10] solve (19) variationally [10, 21] with the Gaussian ansatz (21) and determine the width parameter η via

$$\eta^4 - 2\sqrt{2\pi}\eta a a_z n_2 - 1 = 0. \tag{25}$$

The solution of the nonlinear (25) when substituted into (22) yields the desired $\bar{\mu}_z$ [10] through a procedure far complicated than the analytic formulae (24).

The approximation scheme of MMD is quite involved but does not require the solution of a nonlinear variational equation like SPR. They calculate $\bar{\mu}_z(n_2)$ via [11]

$$\bar{\mu}_z(n_2) = \frac{1}{8}[(\eta + \sqrt{\eta^2 - \zeta^6})^{1/3} + (\eta - \sqrt{\eta^2 - \zeta^6})^{1/3} - \zeta]^2 \tag{26}$$

where $\eta = 4 + 6\zeta - \zeta^3 + 24\pi x$ and $\zeta = (\kappa - 1)$ with

$$\kappa^{-1} = \sqrt{2/\pi} + \Theta(x - 0.1)(1 - \sqrt{2/\pi})[1 - (10x)^{-1/5}] \tag{27}$$

where $x \equiv aa_z n_2$, and the Heaviside step function $\Theta(x - 0.1) = 0$, for $x < 0.1$, and $= 1$ for $x > 0.1$. It is realized that the function (27) is not analytic in x.

Table 2. Chemical potential $\bar{\mu}_z(n_2)$ of (20) for different $aa_z n_2$ obtained from an accurate numerical solution of (19), and from (24) (Present, $\eta = 0.95$), (26) (MMD) [11], and (25) (SPR) [10].

$aa_z n_2$	Numerical	MMD	SPR	Present
0	0.5	0.5	0.5	0.50263
0.2	1.348783	1.31186	1.36149	1.34376
1	3.599892	3.50165	3.69266	3.54355
10	16.45405	16.2547	17.0012	16.3294
100	76.30080	75.9963	78.8855	76.1358

Now we calculate the chemical potential $\bar{\mu}_z(n_2)$ of the three approaches and compare them with the precise result for $\bar{\mu}_z(n_2)$ from a numerical solution of (19). The results are shown in table 2 for different $aa_z n_2$ along with those from the MMD and SPR schemes. After a small experimentation the constant η in (24) was fixed at $\eta = 0.95$ for all $aa_z n_2$.

3. 3D-1D and 3D-2D reductions of Fermi superfluid DF equations

We consider a Gallilei-invariant density-functional (DF) formulation for a trapped Fermi superfluid at BCS and unitarity limits described by [6, 7]

$$\left[-i\hbar\frac{\partial}{\partial\hat{t}} - \frac{\hbar^2\nabla^2_{\hat{\mathbf{r}}}}{4m} + 2V(\hat{\mathbf{r}}) + 2^{2/3}\chi\frac{2\hbar^2}{m}|\Psi(\mathbf{r})|^{4/3}\right]\Psi(\hat{\mathbf{r}}, t) = 0, \tag{28}$$

with $\chi = (3\pi^2)^{2/3}\xi/2$ ($\xi = 1$ at the BCS limit and $\xi = 0.44$ at unitarity [23]), N the number of fermions, and normalization $\int |\Psi|^2 d^3\hat{\mathbf{r}} = N/2$ ($|\Psi|^2$ is the density of Fermi pairs), m the mass of an atom, $V(\hat{\mathbf{r}}) = m\omega^2(\hat{\rho}^2 + \lambda^2\hat{z}^2)/2$ the harmonic trapping potential with frequencies ω and $\lambda\omega$ in radial ($\hat{\rho}$) and axial ($\hat{z}$) directions ($\hat{\mathbf{r}} \equiv \hat{\rho}, \hat{z}$). The fully-paired Fermi superfluid is assumed to be composed of spin-half fermions with an equal number of spin-up and -down components. Employing dimensionless units $t = \hat{t}\omega, \mathbf{r} = \hat{\mathbf{r}}/a_\rho, z = \hat{z}/a_\rho, \rho = \hat{\rho}/a_\rho, a = \hat{a}/a_\rho, \psi\sqrt{N/2} = \Psi a_\rho^{3/2}, a_\rho = \sqrt{\hbar/m\omega}$, (28) can be written as

$$\left[-i\frac{\partial}{\partial t} - \frac{\nabla^2_{\mathbf{r}}}{4} + \rho^2 + \lambda^2 z^2 + 2\chi N^{2/3}|\psi|^{4/3}\right]\psi(\mathbf{r}, t) = 0, \tag{29}$$

with $\int |\psi|^2 d^3\mathbf{r} = 1$($|\psi|^2$ is the density of Fermi atoms).

3.1. 3D-1D reduction for a cigar-shaped Fermi superfluid

For a cigar-shaped trap, we consider the factorization (3). We substitute (3) in (29) and multiply the resultant equation by $\varphi^*(\rho, n_1)$ and integrate in ρ to get

$$\left[i\frac{\partial}{\partial t} + \frac{1}{4}\frac{\partial^2}{\partial z^2} - \lambda^2 z^2 - \mu_\rho(n_1)\right]\phi(z,t) = 0, \tag{30}$$

where $\mu_\rho(n_1)$ is the chemical potential emerging from the following 2D DF equation

$$\left[-\frac{\nabla_\rho^2}{4} + \rho^2 + 2\chi n_1^{2/3}|\varphi|^{4/3} - \mu_\rho(n_1)\right]\varphi(\rho, n_1) = 0. \tag{31}$$

In the small N weak-coupling limit, the wave function $\varphi(\rho, n_1)$ can be approximated by the normalized Gaussian form [21] (8). With this wave form the chemical potential of (31) becomes

$$\mu_\rho(n_1) = \left(\alpha^2 + \frac{1}{4\alpha^2}\right) + \frac{6\chi}{5}\frac{n_1^{2/3}}{\alpha^{4/3}\pi^{2/3}}. \tag{32}$$

Chemical potential $\mu_\rho(n_1)$ of (32) is consistent with (4.7) of AS [20]. In the large N TF limit the normalization condition of the TF wave function leads to [10, 11]

$$\mu_\rho(n_1) = \left[\left(\frac{5n_1}{2\pi}\right)^{2/3} 2\chi\right]^{3/5} \approx 1.38336 n_1^{2/5}\chi^{3/5}. \tag{33}$$

Chemical potential (33) is approximately equal to the chemical potential in the large N limit of the corresponding model (4.10) of AS [20] which yields in present notation

$$\mu_\rho(n_1) = \frac{7}{5}\frac{(6\chi)^{3/5} n_1^{2/5}}{(5\pi^2)^{1/5} 2^{2/5}} \approx 1.42545 n_1^{2/5}\chi^{3/5}. \tag{34}$$

Here we use the following simple interpolation formula for $\mu_\rho(n_1)$ incorporating the limiting values (32) and (33)

$$\mu_\rho(n_1) = \frac{1}{4\alpha^2} - \frac{3\alpha^2}{2} + \left[\left(\frac{5\alpha^2}{2}\right)^{5/3} + 2\chi\left(\frac{5n_1}{2\pi}\right)^{2/3}\right]^{3/5}. \tag{35}$$

where α is taken as a fixed constant for all n_1.

AS [20] solve Eq. (31) variationally and obtain for the width α

$$\alpha^4 = \frac{1}{4} + \frac{12\chi}{25}\left(\frac{n_1\alpha}{\pi}\right)^{2/3}. \tag{36}$$

Here we calculate the chemical potential $\mu_\rho(n_1)$ obtained from (35) for different α and from (4.7) and (4.8) of [20] and compare with the precise result for $\mu_\rho(n_1)$ from a numerical solution of (31). Our finding is exhibited in table 3 for different n_1 together with those from the AS [20] scheme. After a small experimentation it was found that the best overall result from (35) was found for $\alpha = 0.98/\sqrt{2}$.

Now to see how well the effective 1D equations (30) and (35) reproduce the linear density $\phi^2(z)$ of a cigar-shaped Fermi superfluid we plot in figure 1 (a) the 1D density calculated from (30) and (35) and the same calculated from the full 3D (29) for $\lambda = 1/4$ and $N = 2, 10, 100$. The excellent agreement between the two sets of results for λ as large as 1/4 demonstrates the usefulness of the present 1D model equations.

Table 3. Chemical potential $\mu_\rho(n_1)$ of (30) for different n_1 for a Fermi superfluid at unitarity ($\xi = 0.44$) obtained from an accurate numerical solution of (31), from (32) and (36) (AS) [6], and from (35) (Present, $\alpha = 1/\sqrt{2}$, and $0.98/\sqrt{2}$).

n_1	Numerical	AS	Present $\alpha = 1/\sqrt{2}$	Present $\alpha = 0.98/\sqrt{2}$
0	1	1	1	1.00081
0.1	1.37401	1.37619	1.36784	1.37667
1	2.43893	2.46380	2.39751	2.41810
10	5.56376	5.69170	5.45891	5.49147
100	13.70413	14.09704	13.5463	13.5867
1000	34.29934	35.33109	34.1057	34.1506

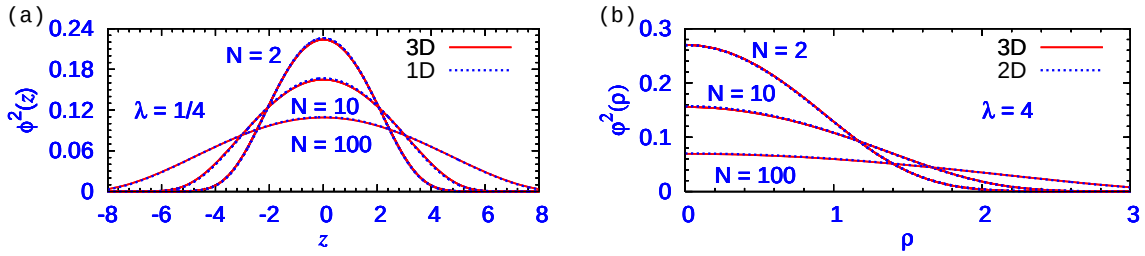

Figure 1. (Color online) (a) The linear density $\phi^2(z)$ of a Fermi superfluid at unitarity (with $\xi = 0.44$) vs. z (both in dimensionless units) calculated from the 3D DF equation (29) and the 1D model (30) and (35) for $\lambda = 1/4, \alpha = 0.98/\sqrt{2}$ and $N = 2$, 10, and 100. (b) The radial density $\varphi^2(\rho)$ of a Fermi superfluid at unitarity (with $\xi = 0.44$) vs. ρ (both in dimensionless units) calculated from the 3D DF equation (29) and the 2D model (37) and (44) for $\lambda = 4, \eta = 0.92/\sqrt{2}$ and $N = 2$, 10, and 100.

3.2. 3D-2D reduction for a disk-shaped Fermi superfluid

In the case of a disk-shaped trap we consider the factorization (14) and substitute it in (29), multiply the resultant equation by $\phi^*(z, n_2)$ and integrate in z to get

$$\left[i\frac{\partial}{\partial t} + \frac{1}{4}\nabla_\rho^2 - \rho^2 - \mu_z(n_2) \right] \varphi(\rho, t) = 0, \tag{37}$$

where $\mu_z(n_2)$ is the chemical potential emerging from the following 1D DF equation

$$\left[-\frac{1}{4}\frac{\partial^2}{\partial z^2} + \lambda^2 z^2 + 2\chi n_2^{2/3}|\phi|^{4/3} - \mu_z(n_2) \right] \phi(z, n_2) = 0. \tag{38}$$

It is convenient to introduce scaled variables $\bar{z} = z/a_z, \bar{\phi} = \sqrt{a}_z\phi$, and $\bar{\mu}_z = \mu_z a_z^2$ with $a_z = \sqrt{1/\lambda}$, when (38) becomes

$$\left[-\frac{1}{4}\frac{\partial^2}{\partial \bar{z}^2} + \bar{z}^2 + 2\chi a_z^{4/3} n_2^{2/3}|\bar{\phi}|^{4/3} - \bar{\mu}_z(n_2) \right] \bar{\phi}(z, n_2) = 0, \tag{39}$$

$$\bar{\mu}_z(n_2) = \int d\bar{z}\bar{\phi}^* \left[-\frac{1}{4}\frac{\partial^2}{\partial \bar{z}^2} + \bar{z}^2 + 2\chi a_z^{4/3} n_2^{2/3}|\bar{\phi}|^{4/3} \right] \bar{\phi}. \tag{40}$$

The form of the chemical potential $\bar{\mu}_z(n_2)$ of (39) is known in the small and large N limits. In the small N weak-coupling limit the wave function $\bar{\phi}(\bar{z}, n_2)$ can be approximated by the normalized Gaussian form [21] (21). With this wave form the chemical potential of (40) becomes

$$\bar{\mu}_z(n_2) = \left(\frac{\eta^2}{2} + \frac{1}{8\eta^2}\right) + \frac{2\chi(n_2 a_z^2)^{2/3}}{\eta^{2/3}\pi^{1/3}}\sqrt{\frac{3}{5}}. \tag{41}$$

Chemical potential $\bar{\mu}_z(n_2)$ of (41) is consistent with (5.7) of AS [20]. In the large N TF limit the normalization condition of the TF wave function leads to [11]

$$\bar{\mu}_z(n_2) = \left[\frac{8\chi n_2^{2/3} a_z^{4/3}}{(3\pi)^{2/3}}\right]^{3/4} \approx 1.54947\chi^{3/4} a_z\sqrt{n_2}. \tag{42}$$

Chemical potential (42) is approximately equal to the chemical potential in the large N limit of the corresponding model (5.10) of AS [20] which yields in present notation

$$\bar{\mu}_z(n_2) = \frac{12 a_z 3^{3/8}\chi^{3/4}\sqrt{n}_2}{5\sqrt{2}\pi^{1/4}5^{1/8}} \approx 1.57383\chi^{3/4} a_z\sqrt{n}_2. \tag{43}$$

Here we use the following interpolation formula for $\bar{\mu}_z(n_2)$ incorporating the limiting values (41) and (42)

$$\bar{\mu}_z(n_2) = \left(\frac{\eta^2}{2} + \frac{1}{8\eta^2}\right) - \frac{15^{3/2}\eta^2}{9\pi} + \left[\left(\frac{15^{3/2}\eta^2}{9\pi}\right)^{4/3} + 8\chi\frac{(n_2 a_z^2)^{2/3}}{(3\pi)^{2/3}}\right]^{3/4}. \tag{44}$$

where η is taken as a fixed constant for all $a_z^2 n_2$.

AS [20] solve Eq. (39) variationally and obtain for the width η

$$\eta^4 = \frac{1}{4} + \frac{4\chi}{5}\frac{(a_z^2 n_2\eta^2)^{2/3}}{\pi^{1/3}}\sqrt{\frac{3}{5}}. \tag{45}$$

Table 4. Chemical potential $\bar{\mu}_z(n_2)$ of (40) for different $a_z^2 n_2$ for a Fermi superfluid at unitarity ($\xi = 0.44$) obtained from an accurate numerical solution of (39), from (41) and (45) (AS) [6], and from (44) (Present, $\eta = 1/\sqrt{2}$ and $\eta = 0.92/\sqrt{2}$).

$a_z^2 n_2$	Numerical	AS	Present $\eta = 1/\sqrt{2}$	Present $\eta = 0.92/\sqrt{2}$
0	0.5	0.5	0.5	0.50696
0.1	1.071781	1.07375	1.05892	1.08883
1	2.79861	2.82290	2.72155	2.78109
10	8.59782	8.72108	8.41456	8.50454
100	27.09534	27.51645	26.8149	26.9282
500	60.56659	61.51645	60.2317	60.3571

As in the 3D-1D reduction, now we calculate the chemical potential $\bar{\mu}_z(n_2)$ of the three approaches and compare them with the precise result for $\bar{\mu}_z(n_2)$ obtained from

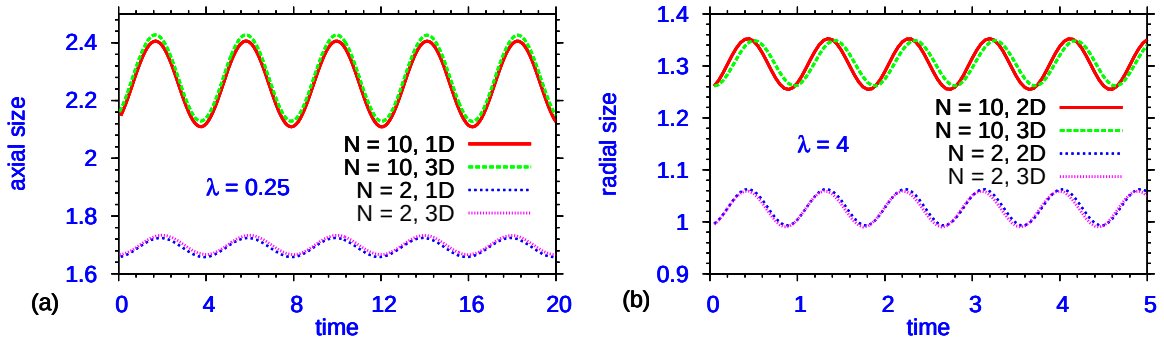

Figure 2. (Color online) (a) The rms axial size vs. time (both in dimensionless oscillator units) during oscillation of a cigar-shaped Fermi superfluid at unitarity ($\xi = 0.44$) for $\lambda = 0.25$, started by reducing the axial trap suddenly by a factor of 0.9, as calculated by the full 3D equation (29) and the reduced 1D equations (30) and (35) for $\alpha = 0.98/\sqrt{2}$. (b) The rms radial size vs. time (both in dimensionless oscillator units) during oscillation of a disk-shaped Fermi superfluid at unitarity for $\lambda = 4$, started by reducing the radial trap suddenly by a factor of 0.9, as calculated by the full 3D equation (29) and the reduced 2D equations (37) and (44) for $\eta = 0.92/\sqrt{2}$.

a numerical solution of (39). The results are shown in table 4 for different $a_z^2 n_2$ along with those from the AS scheme [20].

Now to see how well the effective 2D equations (37) and (44) reproduce the radial density $\varphi^2(\rho)$ of a disk-shaped Fermi superfluid we plot in figure 1 (b) the 2D density calculated from (37) and (44) and the same calculated from the full 3D (29) for $\lambda = 4$ and $N = 2, 10, 100$. The excellent agreement between the two sets of results for λ as small as 4 demonstrates the usefulness of the present 2D model equations.

3.3. Dynamics: Breathing oscillation

Now we subject the reduced 1D and 2D DF equations to a more stringent test, e.g., how well these equations can reproduce non-stationary (non-equilibrium) dynamics of a cigar- and disk-shaped Fermi superfluid. First we consider a cigar-shaped Fermi superfluid with $\lambda = 0.25$, which is set into breathing oscillation by reducing only the axial potential suddenly by a factor of 0.9. The radial trap is left unchanged. The resultant oscillation is studied using the full 3D DF equation (29) as well as the reduced 1D DF equation (30) using the chemical potential (35). The root mean square (rms) axial size as calculated from the 3D and 1D equations are plotted in figure 2 (a). Next we consider a disk-shaped Fermi superfluid with $\lambda = 4$, which is set into breathing oscillation by reducing only the radial potential suddenly by a factor of 0.9. The resultant oscillation is studied using the full 3D DF equation (29) as well as the reduced 2D DF equation (37) using the chemical potential (44). The rms radial size as calculated from the 3D and 2D equations are plotted in figure 2 (b).

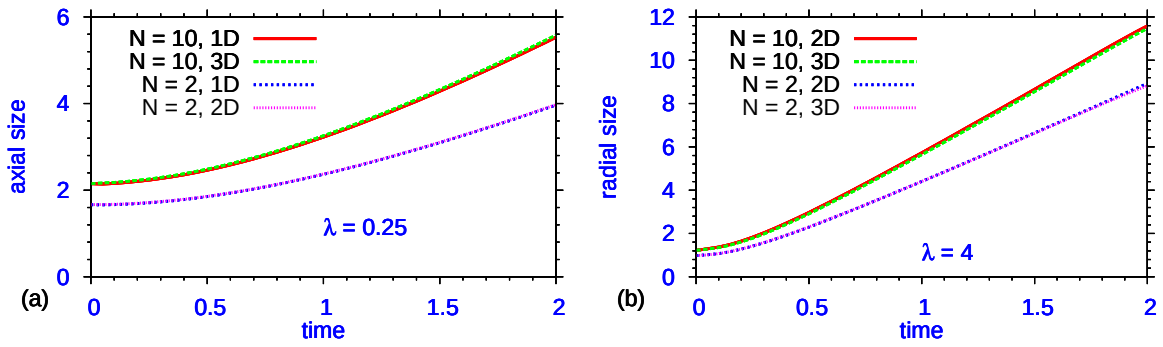

Figure 3. (Color online) (a) The rms axial size vs time (both in dimensionless oscillator units) during axial expansion of a cigar-shaped Fermi superfluid at unitarity ($\xi = 0.44$) for $\lambda = 0.25$, started by removing the axial trap suddenly, as calculated by the full 3D equation (29) and the reduced 1D equations (30) and (35) for $\alpha = 0.98/\sqrt{2}$. (b) The rms radial size vs time (both in dimensionless oscillator units) during radial expansion of a disk-shaped Fermi superfluid at unitarity for $\lambda = 4$, started by removing the radial trap suddenly, as calculated by the full 3D equation (29) and the reduced 2D equations (37) and (44) for $\eta = 0.92/\sqrt{2}$.

3.4. Dynamics: Free expansion

Now we consider the problem of free expansion of a cigar- and disk-shaped Fermi superfluid, respectively, when the axial and radial traps are suddenly removed after the formation of the superfluid. First we consider a cigar-shaped Fermi superfluid with $\lambda = 0.25$ which is allowed to expand freely in the axial direction by setting the axial trap suddenly to zero in the 3D equation. The radial trap is left unchanged. The resultant expansion is studied using the full 3D DF equation (29) as well as the reduced 1D DF equation (30) using the chemical potential (35). The rms axial size as calculated from the 3D and 1D equations are plotted in figure 3 (a). Next we consider a disk-shaped Fermi superfluid with $\lambda = 4$, which is allowed to expand freely in the radial direction by setting the radial trap suddenly to zero in the 3D equation. The axial trap is left unchanged. The resultant expansion is studied using the full 3D DF equation (29) as well as the reduced 2D DF equation (37) using the chemical potential (44). The rms radial size as calculated from the 3D and 2D equations are plotted in figure 3 (b). The agreement between the dynamics as obtained from the full 3D DF equation and that from the reduced DF equations in Figs. 2 and 3 is quite satisfactory.

4. Conclusion

In conclusion, we have suggested time-dependent mean-field reduced DF equations in 1D and 2D, respectively, for a cigar- and disk-shaped BEC and Fermi superfluid in the BCS and unitarity limits with simple analytic nonlinear terms. The numerical solution of these reduced equations reveals that they produce results for density of Fermi superfluids and BEC in cigar- and disk-shaped traps in excellent agreement with the solution of the

full 3D DF equation. We also studied non-stationary breathing oscillation of the cigar- and disk-shaped Fermi superfluid initiated by a sudden change of axial and radial traps, respectively. Finally, we applied the reduced equations to the study of free expansion of a cigar- and disk-shaped Fermi superfluid initiated by a sudden removal of the axial and radial trap, respectively. The reduced equations produced equally good results in both these studies when compared with the solution of the full 3D equations.

Acknowledgments

FAPESP, CAPES and CNPq (Brazil) provided partial support.

References

[1] Dalfovo F, Giorgini S, Pitaevskii L and Stringari S 1999 *Rev. Mod. Phys.* **71** 463
[2] Eagles D M 1969 *Phys. Rev.* **186** 456
Leggett A J 1980 *J. Phys. (Paris) Colloq.* **41** C7-19
Adhikari S K *et al.* 2000 *Phys. Rev. B* **62** 8671
[3] Giorgini S, Pitaevskii L and Stringari S 2008 *Rev. Mod. Phys.* **80** 1215
[4] Greiner M , Regal C A and Jin D S 2003 *Nature* **426** 537
Kinast J, Hemmer S L, Gehm M E, Turlapov A and Thomas J E 2004 *Phys. Rev. Lett.* **92** 150402
[5] Zwierlein M W *et al.* 2004 *Phys. Rev. Lett.* **92** 120403
Zwierlein M W, Schunck C H, Stan C A, Raupach S M F and Ketterle W 2005 *Phys. Rev. Lett.* **94** 180401
[6] Adhikari S K and Salasnich L 2008 *Phys. Rev. A* **78** 043616
[7] Adhikari S K 2009 *Phys. Rev. A* **79** 023611
[8] Blume D, von Stecher J and Greene C H 2007 *Phys. Rev. Lett.* **99** 233201
Chang S Y and Bertsch G F 2007 *Phys. Rev.* A **76** 021603(R)
[9] Görlitz A *et al.* 2001 *Phys. Rev. Lett.* **87** 130402
[10] Salasnich L, Parola A and Reatto L 2002 *Phys. Rev. A* **65** 043614
[11] Muñoz Mateo A and Delgado V 2008 *Phys. Rev. A* **77** 013617
[12] Salasnich L, Parola A and Reatto L 2004 *Phys. Rev. A* **69** 045601
[13] Muñoz Mateo A and Delgado V 2007 *Phys. Rev. A* **75** 063610
[14] Jackson A D, Kavoulakis G M and Pethick C J 1998 *Phys. Rev.* A **58** 2417
[15] Chiofalo M L and Tosi M P 2000 *Phys. Lett.* A **268** 406
[16] Massignan P and Modugno M 2003 *Phys. Rev. A* **67** 023614
[17] Kamchatnov A M and Shchesnovich V S 2004 *Phys. Rev. A* **70** 023604
[18] Zhang W and You L 2005 *Phys. Rev. A* **71** 025603
[19] Abdullaev F K and Galimzyanov R 2003 *J. Phys. B: At. Mol. Opt. Phys.* **36** 1099
[20] Adhikari S K and Salasnich L 2009 *New J. Phys.* **11** 023011
[21] Pérez-García V M, Michinel H, Cirac J I, Lewenstein M and Zoller P 1997 *Phys. Rev. A* **56** 1424
[22] Adhikari S K and Muruganandam P 2009 *Comput. Phys. Commun.* **180** 1888
[23] Astrakharchik G E *et al.* 2004 *Phys. Rev. Lett.* **93** 200404
Carlson J *et al.* 2003 *Phys. Rev. Lett.* **91** 050401